Toxicity and antimicrobial properties of ZnO@ZIF-8 embedded silicone against planktonic and biofilm catheter-associated pathogens

James Redfern,[†] Lisa Geerts,[‡] Jin Won Seo,[±] Joanna Verran,[†] Lubomira Tosheva,[*,†] and Lik H. Wee[*,‡]

[†]Faculty of Science and Engineering, Manchester Metropolitan University, Chester Street, Manchester M1 5GD, United Kingdom

[‡]Centre for Surface Chemistry and Catalysis, University of Leuven, Celestijnenlaan 200f, B3001, Heverlee, Leuven, Belgium

[±]Department of Materials Engineering, University of Leuven, Kasteelpark Arenberg 44, B3001 Leuven, Belgium

ABSTRACT A ZnO@ZIF-8 powder on a gram scale was prepared via treatment of ZIF-8 with silver nitrate to induce spontaneous formation of ZnO nanorods on the surface of the ZIF-8 crystals. The crystal structure, phase purity and physicochemical characteristics of ZnO@ZIF-8

1

were determined by X-ray diffraction, high resolution electron microscopy, energy dispersive spectroscopy and nitrogen adsorption. The antimicrobial potential of ZnO@ZIF-8 for reduction of microorganisms often implicated with catheter-associated urinary tract infections (CAUTIs) was studied in detail using four target pathogens, *Escherichia coli*, *Klebsiella pneumoniae*, *Proteus mirabilis* and *Staphylococcus aureus*. The ability of the compound to kill all four microorganisms in suspension was established and a minimum bactericidal concentration of 0.25 mg mL^{-1} was determined for each microorganism. ZnO@ZIF-8 compound was found to be no more toxic to *Galleria mellonella* than distilled water, which was assessed by injection of *Galleria* with 10 µL of ZnO@ZIF-8 of concentrations of up to 2 mg mL^{-1}. ZnO@ZIF-8 suspensions (2 mg mL^{-1} concentration) were able to reduce well-established biofilms of all four oraganisms containing between 10^7 and 10^9 CFU mL^{-1} to below limit of detection (BLD) over a 24-h period. Silicone-embedded ZnO@ZIF-8 (2wt.% or 4 wt.% ZnO@ZIF-8 loading) also demonstrated antimicrobial properties with all four microorganisms being eliminated from the surface within 24 h. The ZnO@ZIF-8 high potency and rapid anti-biofilm activity against all four test organisms coupled with its non-toxicity offers a new avenue for control of microbial colonization of catheters, which would ultimately result in reduction of CAUTIs.

1. INTRODUCTION

Urinary tract infections (UTIs) are the fourth most common healthcare-associated infection in US hospitals,[1] with upwards of 70% of UTIs being linked to catheterization of a patient.[2] Catheters pose a significant risk as a microbial reservoir due to the often prolonged use and flow of nutrient-rich liquids combined with the ability of microorganisms to adhere to the surface and grow complex communities (biofilm), leading to colonization of the catheter. Biofilms linked

with catheter-associated urinary tract infections (CAUTIs) are able to resist antimicrobial activity, and often cause catheter blockages, with the risk of bacteremia increasing by three to seven percent everyday a patient is catheterized.[3] CAUTIs can be caused by a number of potentially pathogenic microorganisms, with *Escherichia coli*, *Klebsiella pneumoniae*, *Proteus mirabilis* and *Staphylococcus aureus* being commonly isolated from colonized catheters.[4] These bacteria are also included on the WHO Priority Pathogens list relating to the most clinically significant antimicrobial resistant microorganisms.[5]

Although common strategies to control microbial colonization of catheters such as aseptic handling and reduced catheterization time are beneficial, alterations to the catheter material may also provide benefits. Currently, the majority of catheters are made of plastics or latex.[6] However, attempts have been made to modify these materials to include biocides and other antimicrobial compounds such as hydrogels, lecithin, silver-coatings and impregnation with compounds such as antibiotics, essential oils or nitric oxide.[6-12] Various meta-analyses of studies into the efficacy of antimicrobial catheters have shown their potential for reducing infections.[13,14]

Metal-organic frameworks (MOFs) are a relatively new class of inorganic-organic hybrid materials constructed via covalent bonding of metal ions/clusters with the polydentate bridging ligands.[15] Due to their structural diversity, excellent permanent porosity, tunable pore size and high chemical functionality, MOFs have shown their potential use for a vast range of applications ranging from gas storage,[16,17] separation,[18] catalysis,[19] and chemical sensing[20] to advanced biomedicine,[21,22] drug delivery and bioimaging.[23] Combining the tailorability of the MOF with the versatile functionality of metal oxide nanoparticles (e.g. TiO_2, ZnO, and Ag_2O) with novel physicochemical properties are particularly attractive for the fundamental search of emerging potential applications in the field of advanced nanotechnology, such as solar cell,

selective sensing, separation and photocatalysis.[24-29] For example, ZnO@ZIF-8 core-shell

nanostructures have shown selective photoelectrochemical response to H_2O_2, excluding the

bulkier interfering chemicals such as ascorbic acid present in the buffer solution.[30] ZnO@ZIF-8

core-shell heterostructure has also been reported as promising photocatalyst for selective

reduction of Cr(VI) between Cr(VI) and methylene blue.[31] In these systems, the ZnO nanorods

not only act as the template but also provide Zn^{2+} ions for the formation of ZIF-8 in 2-

methylimidazolate solution via solvothermal treatment.[30,31]

Alternatively, we have successfully demonstrated a spontaneous phase segregation of ZIF-8

into ZnO nanorods upon exposure of ZIF-8 nanocrystals to an aqueous solution of silver nitrate

at room temperature (Scheme 1).[32] ZnO@ZIF-8 composite is photocatalytically active for the

photodegradation of methylene blue.[32] ZnO nanorod having a band-gap energy of 3.16 eV has

attracted much attention due to its unique optical, electrical and chemical properties, making it an

ideal nanomaterial for optoelectronics, piezoelectric generators and biotechnology.[32,33] The

antibacterial behavior of ZnO nanoparticles has been documented in the literature.[34,35] Inspired

by the long-term broad spectrum antibacterial activity of ZnO nanoparticles, the fabrication of

multifunctional ZnO@ZIF-8 nanocomposite could be useful for biomedical applications.

Moreover, thanks to the inorganic-organic hybrid property of MOF, it allows facile processing of

MOF-based composite materials into application-specific configurations, such as mixed matrix

membranes due to the excellent chemical compatibility between the MOF filler and the polymer

phase.[36,37] In this study, we show laboratory upscaling synthesis of a gram-scale ZnO@ZIF-8

nanocomposite and its potential application as biofilm inhibitor to prevent colonization by

common pathogens associated with urinary tract infection. More importantly, we also

demonstrate the incorporation of ZnO@ZIF-8 nanocomposite into silicone elastomers to form

self-supporting composite material with high antimicrobial property against catheter-associated urinary tract infection pathogens.

Scheme 1. Schematic representation the spontaneous local transformation of pre-synthesized ZIF-8 into nanocomposite of ZIF-8 with embedded ZnO nanorods induced by silver nitrate solution at room temperature.
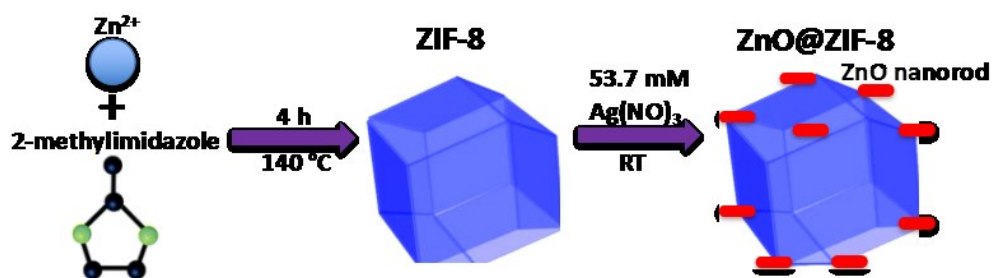
2. EXPERIMENTAL SECTION

2.1. Gram-scale synthesis of ZnO@ZIF-8. 11.75 g of $Zn(NO_3)_2 \cdot 6 H_2O$ (ACROS Organic) was dissolved in 200 mL of dimethylformamide (DMF, ACROS Organic) and 25.92 g of 2-methylimidazole (ACROS Organic) was dissolved in 200 mL of DMF. The 2-methylimidazole solution was added to the zinc nitrate solution under vigorous stirring for 5 min. Spontaneous precipitation was observed after mixing. The mixture was poured into a 2 L SCHOTT bottle (DURAN) and heated at 140 °C for 4 h in an oven. The product was recovered and washed with DMF through repeated centrifugation and redispersion in an ultrasonic bath. Solvent exchange was performed with absolute ethanol (200 mL) (Fisher Chemical) three times over three days. The product was dried in an oven at 80 °C. 1.0 g of ZIF-8 powder was dispersed in an aluminium foil-covered glass bottle containing 35 mL of 53.7 mM silver nitrate (ACROS Organic) Milli-Q

ultrapure water:ethanol (v/v= 1:6) solution and stirred overnight. The solid was washed with absolute ethanol (200 mL) two times and dried at room temperature.

2.2 Characterization of ZnO@ZIF-8. ZnO@ZIF-8 was characterized by a powder X-ray diffractometer (XRD, STOE StadiP diffractometer in high-throughput transmission mode employing Cu Kα1 radiation), N_2 adsorption instrument (Micromeritics Tristar 3000); sample was activated at 150 °C under nitrogen flow overnight prior to measurement, and a Nova Nano scanning electron microscope NanoSEM450 (FEI, Eindhoven). Bright field TEM (BF-TEM), high resolution TEM (HR-TEM) and energy-dispersive X-ray spectroscopy (EDX) were performed with a probe-corrected transmission electron microscope (ARM200F cold-FEG, JEOL) operated at acceleration voltage of 200 kV. TEM samples were prepared by dispersing the powder in 2-propanol and placing a few drops of the solution onto the copper TEM grids covered with lacey carbon film (Pacific Grid Tech, USA).

2.3. Maintenance and standardization of microorganisms. *Escherichia coli* (*E. coli*, NCTC 9001), *Klebsiella pneumoniae* (*K. pneumoniae*, NCTC 13368), and *Staphylococcus aureus* (*S. aureus*, NCTC 6571) were maintained on Luria-Bertani (LB) agar (BD, Sparks, MD), and *Proteus mirabilis* (*P. mirabilis*, NCTC 60) was maintained on cystine lactose electrolyte deficient (CLED) agar (Oxoid, Basingstoke), at 4 °C. For the 'minimum bactericidal concentration' assay, 2-4 colonies of each culture were inoculated into 100 mL of Mueller-Hinton (MH) broth independently and grown 22 ± 1 h at 37 °C with agitation (180 rpm). Cells were harvested by centrifugation (3600 rpm, 10 min) and resuspended in MH broth to an optical density of 0.025 at 600 nm (Jenway 6305 Spectrophotometer, UK) resulting in a suspension concentration of $3.11 \pm 0.3 \times 10^6$ CFU mL^{-1}. For 'assessment of antimicrobial efficacy of ZnO@ZIF-8-containing silicone elastomers' and 'efficacy of ZnO@ZIF-8 as an antibiofilm

agent' assays, 2-4 colonies were inoculated into 100 mL of LB broth and grown at 22 ± 1 h at 37

°C with agitation (180 rpm). Cells were harvested by centrifugation (3600 rpm, 10 min), washed

once in 0.85% NaCl (Oxoid), and resuspended in 0.85% NaCl to optical density 1.0 at 540 nm

resulting in a suspension concentration of $1.87 ± 0.51$x10^8 CFU mL^{-1}.

2.4. Minimum bactericidal concentration (MBC) assay. MBC assays are used as a screen to

determine the minimum amount of an antimicrobial compound that is sufficient to reduce

bacterial survival in liquid culture. For the purpose of this study, the MBC was considered the be

the smallest concentration of a compound that was capable of killing all cells (i.e. zero cells

recovered on agar). The following suspensions were tested: ZIF-8 powder suspended in sterile

distilled water to a concentration of 4 mg mL^{-1}, ZnO (20wt.% nanoparticle suspension in H$_2$O,

particle size < 100 nm, Sigma-Aldrich) suspended in sterile distilled water to a concentration of 6

mg mL^{-1} and ZnO@ZIF-8 powder suspended in sterile distilled water to a concentration of 4 mg

mL^{-1}. A doubling dilution was then performed in a 96-well plate down to a concentration of

0.0625 mg mL^{-1} for ZIF-8 and ZnO@ZIF-8 and 0.05 mg mL^{-1} for ZnO, leaving a 100 μL volume

of each dilution in its corresponding well. 100 μL of standardized *E. coli* in MH broth (as

described above) was put into each well and incubated and covered with lid, at 37 °C for 18 h.

100 μL of culture plus 100 μL of sterile distilled water was used as a positive control and 100 μL

of suspended ZnO@ZIF-8 plus 100 μL of sterile distilled water was used as a negative control.

20 μL samples were taken from each well after mixing of each well with the pipette, pipetted

onto LB agar, and incubated for 24 h at 37 °C. The lowest concentration at which growth was

prevented was recorded as the MBC. Three independent replicates were tested in each

experiment and the experiment was repeated once for the three remaining bacterial strains.

2.5. Toxicity of ZnO@ZIF-8 using the model *Galleria mellonella*. *G. mellonella,* in the caterpillar larvae stage, are 2-2.5 cm long and cream in color. They can be used as a model for infection and toxicity.[38] *G. mellonella* (Livefood UK Ltd, Somerset) were injected with 10 μL of 2 mg mL^{-1}, 1 mg mL^{-1}, 0.5 mg mL^{-1} and 0.25 mg ml^{-1} of ZnO@ZIF-8 powder suspended in sterile distilled water using a 22 gauge needle (Hamilton Company, Reno) and repeating dispenser syringe (Hamilton Company). Target injection site was the rear left proleg. Ten *Galleria* per experimental condition were used. *Galleria* were incubated at 37 °C for 96 h. Change from the standard creamy color to black and non-motile was indicative of death and assessed every 24 h. Each experiment was repeated once.

2.6. Efficacy of ZnO@ZIF-8 as an antibiofilm agent. MBEC^{TM} biofilm assay plate are designed to establish a biofilm on one of ninety-six pegs, each of which sit within a well. Once a biofilm is established, the pegs can be transferred into another well containing an antimicrobial agent, with resulting antimicrobial action determined by counting colonies.[39] In order to establish a biofilm, 200 μL of a 1:100 dilution of bacteria in fresh LB broth was placed in the wells of a MBEC^{TM} biofilm assay plate (Innovotech, Edmonton). Lid with attached pegs was replaced and plates incubated for 48 h at 37 °C in an orbital shaker (110 rpm). LB broth from wells was replaced with fresh LB broth after 24 h. To assess the antimicrobial efficacy against the established biofilms, 200 μL of ZnO@ZIF-8 suspended in sterile distilled water was placed in the wells of a fresh 96-well plate, at concentrations of 2 mg mL^{-1}, 1 mg mL^{-1} and 0.5 mg mL^{-1}, using sterile distilled water as a negative control. The MBEC^{TM} biofilm assay plate lid (containing the pegs with established biofilms) was then placed into the wells containing the ZnO@ZIF-8 suspension, and incubated for 24 h at 37 °C in an orbital shaker (110 rpm). Following incubation with the ZnO@ZIF-8 suspension, MBEC^{TM} assay lid with attached pegs

was removed and gently washed twice in sterile distilled water. 200 µL of sterile distilled water was then placed in wells of a fresh 96-well plate, into which the MBEC^{TM} assay lid was placed, and cells were removed from pegs into the wells by placing the plate and lid in a sonicating water bath (Sonicor, Copiague, NY) for 20 min. The resultant bacterial suspension was then diluted 10-fold (100 µL into 900 µL of sterile physiological saline), to 10^{-7}. 100 µL of each dilution was pipetted in duplicate onto LB agar (CLED was used for *P. mirabilis*) and spread evenly across the agar surface. Plates were incubated for 18 h at 37 °C, after which the number of colonies was counted to calculate CFU mL^{-1}. Time points sampled were 0, 3, 8, and 24 h. All microorganisms were tested over four biofilms (i.e. four pegs) per time point, the experiment as a whole was repeated once.

2.7. Assessment of antimicrobial efficacy of ZnO@ZIF-8-containing silicone elastomers. Silicone elastomers (SE) were prepared from samples of M511 maxillofacial material (Technovent, UK), comprising of a mixture consisting of 29.106 g of Part A (Silicone polymer with Si-H groups) and 3.234 g of part B (vinyl functionalized dimethyl silicone polymer, plus Pt catalyst) according to the manufacturer's instructions. The system components were mixed for 60 s under vacuum using Multivac 4 (Degussa AG, Germany). After a resting time of 15 min, the uncured SE was spread into a 13 cm x 13 cm x 1 cm metal mold using a pallet knife. The mold was placed on a vibrating table for 10-15 min to bring the air bubbles to the surface and the bubbles were burst using a thin wire. The molding was cured at 100 °C for 1 h. After curing, the SE was removed from the steel mold, cut into 1x1 cm pieces and stored in a polythene bag. A melinex sheet was used in the mold to ease the recovery of the cured SE. ZnO@ZIF-8-containing silicone elastomers were prepared similarly after adding either 2 or 4 wt.% ZnO@ZIF-8 to the uncured SE mixture. To assess their antimicrobial potential against the four

test organisms described above, pieces of SE were inoculated with 10 μL of washed and standardized cell suspension, and a 1x1 cm piece of polyethylene (SLS, Nottingham) was placed gently on top. Coupons where placed in a petri dish inside a humid container and incubated at 37 °C. At the appropriate sample time, the SE coupon with PE sheet was dropped into 10 mL of neutralizing buffer (15 g Tween80 (Sigma- Aldrich, Dorset) and 30 g Soya Lecithin (Optima Healthcare Lecithin, Holland and Barrett, UK) dissolved in 1 L of distilled water,[40] vortex-mixed for 30 s to remove the polyethylene from SE and remove any cells from the surface into the liquid. The neutralizing buffer was included to halt any antibacterial action of ZnO@ZIF-8 at the appropriate time point. The resultant bacterial suspension was then diluted 10-fold (1 mL into 9 mL of sterile physiological saline), seven times, to a concentration of 10^{-7} of the original suspension. 100 μL of each dilution was pipetted out in duplicate onto LB agar (CLED was used for *P. mirabilis*) and spread evenly across the agar surface. Plates were incubated for 18 h at 37 °C, after which the number of colonies was counted to calculate CFU mL^{-1}. Time points sampled were 0, 3, 8, and 24 h. All silicone samples were duplicated and the experiment was repeated as a whole once.

2.8. Growth of biofilm for SEM studies

SE were prepared, as described in 2.7, and cut into 1x1cm pieces. The four target pathogens were grown as described in method section 2.3, and resuspended in LB broth to an optical density of 1.0 at 540 nm. SE pieces were placed in a 12-well plate and immersed in one of the test pathogens and incubated, stationary, at 37 °C for 48 h. SE were then removed, washed gently with sterile distilled water and fixed in 4% glutaraldehyde (sample fully submerged in 25 mL) at 4 °C for 12 h. Samples were then removed from fixative and an ethanol gradient was

completed as follows: 30% EtOH for 10 min, 50% EtOH for 10 min, 70% EtOH for 10 min, 90% EtOH for 10 min and 100% EtOH for 10 min, all at room temperature. SE were mouted to SEM stubs and coated with gold priot to SEM analysis. The SEM analysis was performed with a Carl Zeiss Ltd 40VP Supra scanning electron microscope.

3. RESULTS AND DISCUSSION

3.1. Characterization of ZnO@ZIF-8. The crystal structure and the phase purity of ZnO@ZIF-8 were confirmed by XRD. The XRD pattern of ZnO@ZIF-8 (Fig. 1b) reveals additional characteristic diffraction peaks of 31.76, 36.17, 45.71 and 56.54 at 2θ values, which are corresponding to the crystallographic planes of (010), (011), (012) and (110), assigned to ZnO, in additional to the XRD fingerprint which is corresponding to the sodalite zeolitic topology (Fig. 1a).[32,41] No other diffraction peak is observed which confirms the phase purity of ZnO@ZIF-8 composite. It should be mentioned that in our firstly synthesized ZnO@ZIF-8 sample, the composite contained a small amount of impurity.[32] In this study, we have successfully obtained a phase-pure ZnO@ZIF-8 sample through repeated washing with absolute ethanol. The permanent porosity of ZnO@ZIF-8 sample was confirmed by nitrogen physisorption analysis as shown in Fig. 1c. The ZnO@ZIF-8 composite has a respective specific BET surface area and a micropore volume of 1112 $m^2\ g^{-1}$ and 0.50 $cm^3\ g^{-1}$. The presence of the ZnO nanoparticles is confirmed by high-resolution SEM (HRSEM) imaging. Fig. 1d shows that the ZIF-8 crystals have a clear enrichment of ZnO near to the surface as indicated by arrows. The observed contrast between the ZnO nanorods and ZIF-8 crystals in the HRSEM image is known due to the mass thickness sensitivity.[42,43] Fig. 1d allocates clearly the ZIF-8 crystals with regions of surface enrichment, showing the presence of 80-90 nm-sized ZnO particles, homogeneously distributed on the surface of ZIF-8 crystals.
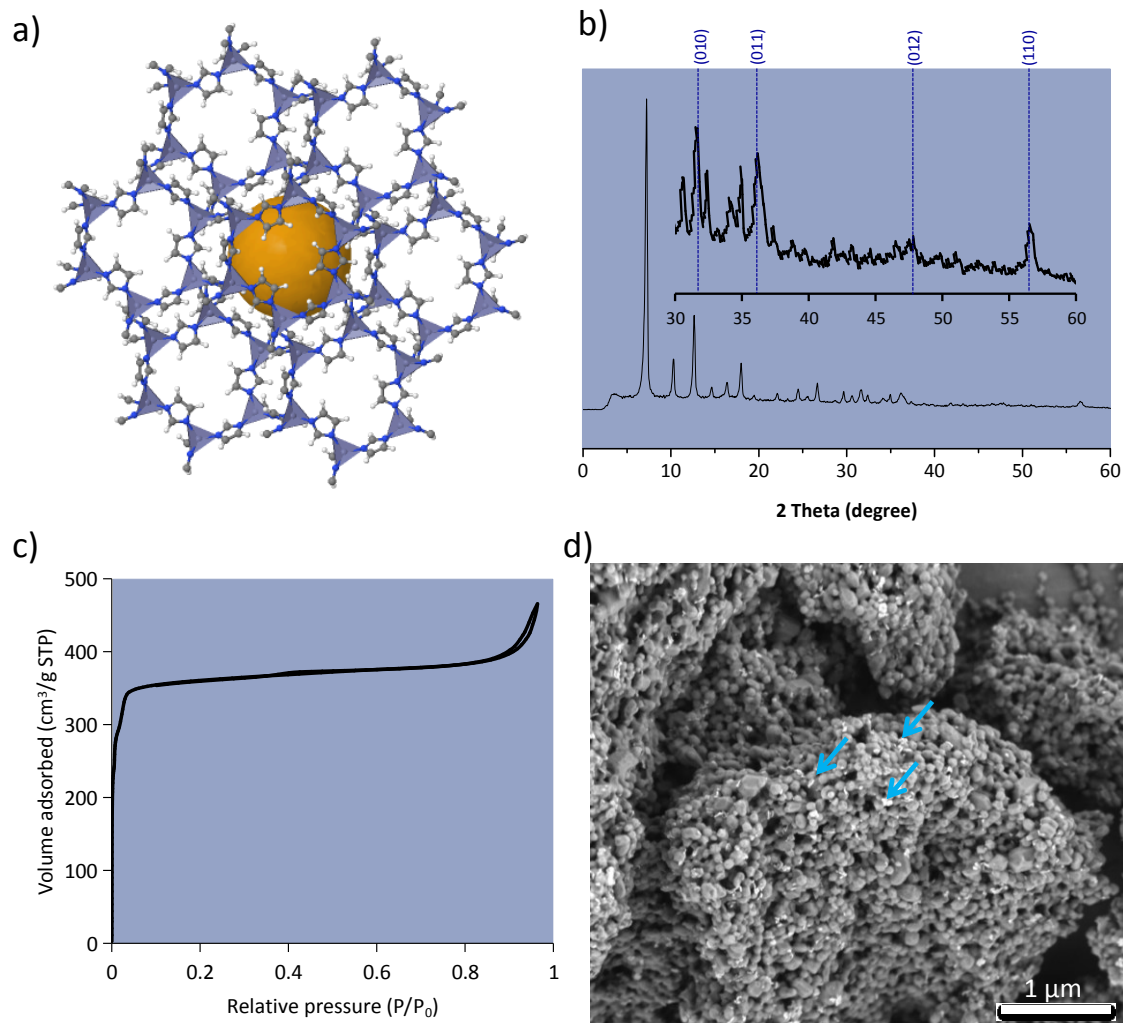
11

Figure 1. (a) The chemical structure of ZIF-8. The blue tetrahedra show the zinc-nitrogen bonds. The orange sphere represents the open-pore structure of ZIF-8. Characterization of ZnO@ZIF-8 by (b) XRD, (c) nitrogen physisorption and (d) HRSEM. The arrows in (d) show the enrichment of ZnO nanorods.

The structural morphology and elemental composition of ZnO@ZIF-8 were characterized in detail by TEM and EDX. Fig. 2 (a-c) shows the BF-TEM images of the synthesized ZnO@ZIF-8 nanocomposite at different magnifications. The small ZnO nanorods (visible as elongated

structures with darker contrast) are evenly distributed on the surface of the ZIF-8 as is visible in

Fig. 2a. HR-TEM image is used to further confirm the presence of ZnO nanorods in ZnO@ZIF-8

nanocomposite. The HR-TEM image (Figure 2d) shows the lattice fringes of ZnO and confirms

the crystallinity of the nanorods. Fig. 2e shows the corresponding fast Fourier transformation

(FFT) analysis. The lattice spacing values are calculated to be 0.52, 0.25 and 0.28 nm in

agreement with the spacing of the (001), (101) and (100) crystalline plane of the ZnO phase,

respectively. Accordingly, the zone axis is parallel with the [010] axis of ZnO. The FFT pattern

is consistent with the XRD results. The EDX spectrum of ZnO@ZIF-8 composite shown in Fig.

2f asserts the presence of carbon (C), nitrogen (N), oxygen (O), zinc (Zn) and copper (Cu)

elements. The presence of C, N and Zn is in agreement with the chemical composition of ZIF-8.

The Cu signal is due to the Cu TEM grid.The absence of any other elements in the EDX

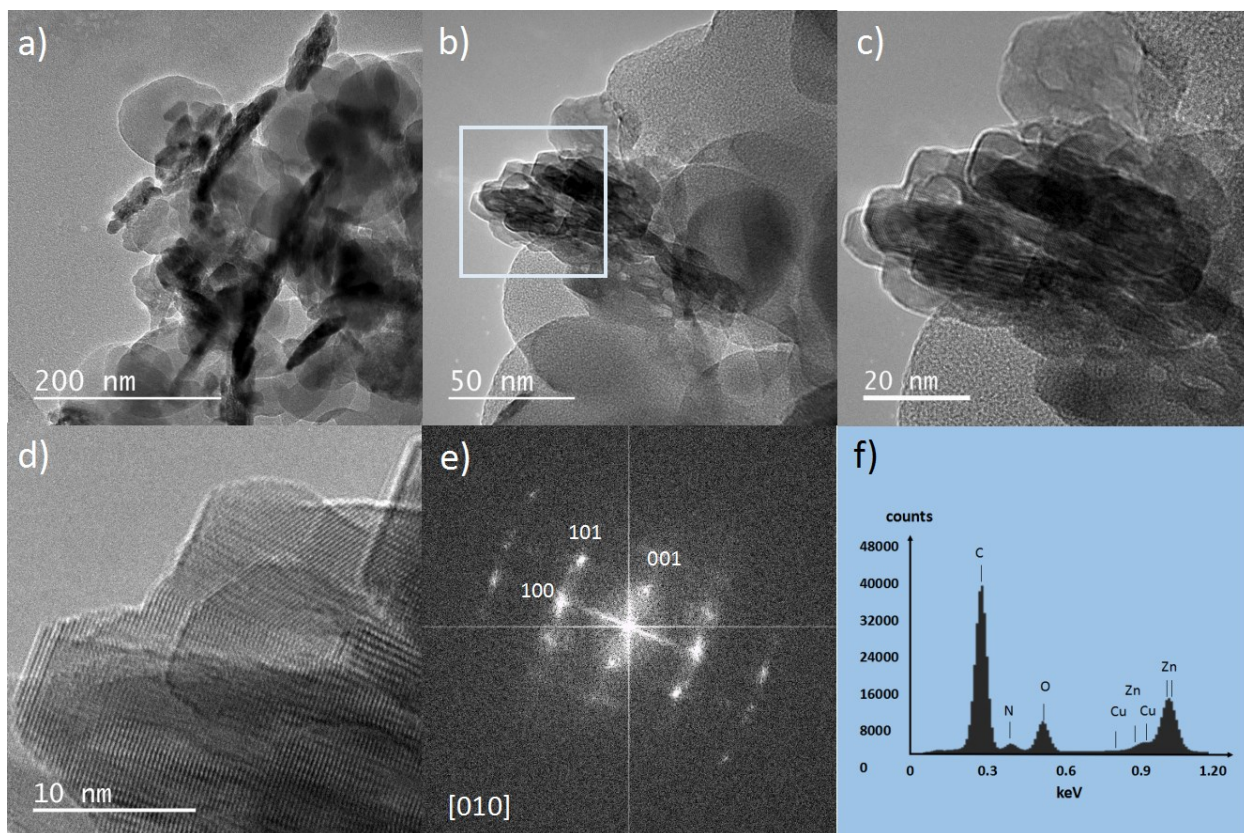spectrum suggests the phase purity of the synthesized ZnO@ZIF-8.

Figure 2. (a, b and c) BF-TEM image of the ZnO@ZIF-8 sample at different magnifications, (c) is the BFTEM image of indicated area in (b) at higher magnification; (d) HR-TEM of the ZnO nanorods and (e) corresponding fast FFT analysis of ZnO nanorods, which confirms a lattice spacing of 0.28 nm for (100) planes and 0.52 nm for (001) planes. These d-spacings are in agreement with the ZnO structure. The zone-axis was found to be [010] direction. (f) EDX spectrum taken from the ZnO@ZIF-8 composite.

3.2. **MBC assay and toxicity assay using the model *Galleria mellonella*.** The lowest concentration that ZnO was able to kill each of the test organisms (MBC) was 0.8 mg mL^{-1}, whilst the ZIF-8 compound exhibited no bactericidal affect. The MBC of ZnO@ZIF-8 was 0.25 mg mL^{-1}for each of the four test organisms. Lower concentrations were unable to kill the test organisms. It has also been reported that the ZnO-loaded polydimethylsiloxane was not active

against *E. coli* and *S. aureus* under dark conditions.[44] This data demonstrates that the ZnO@ZIF-8 compound exhibits greater antimicrobial action against the four test organisms than either ZnO or ZIF-8 alone. Moreover, due to hybrid inorganic-organic nature of ZIF-8 compound, the fixation of ZnO nanorods into the matrix of ZIF-8 helps to enhance the dispersibility of inorganic ZnO nanoparticles, which makes them benefitial as compatible additives to polymers compared to ZnO (Fig. 3). The excellent biocompatibility between the MOF-nanocomposite and polymer is of significant importance for future fabricating of implantable medical devices such as intravascular catheters, urinary catheters and others.[45]
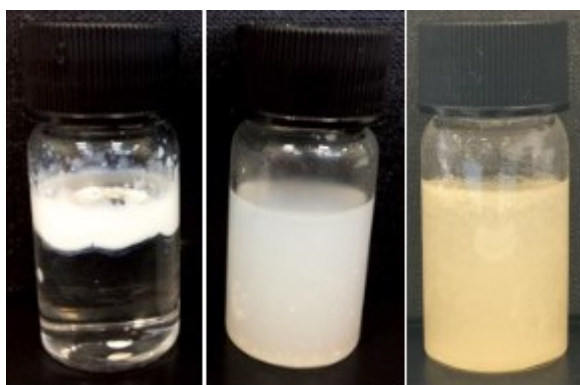

Figure 3. Digital images of samples dispersed in chloroform: (left) ZnO, (middle) ZIF-8 and (right) ZnO@ZIF-8. The photograph was originally taken by LT.
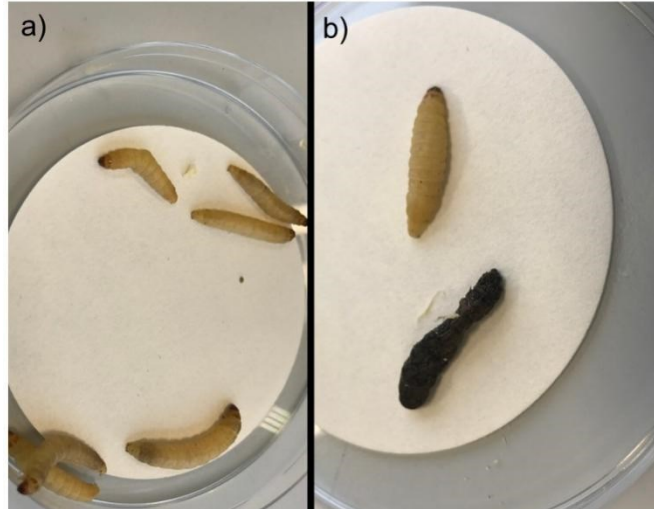
Figure 4. a) Living Galleria mellonella. b) Top larvae is alive (cream in colour) and the bottom larvae is dead (black in colour). The photograph was originally taken by JR. Images presented here are for demonstration purposes and do not represent specific data.

Galleria mellonella, a wax-worm moth used as a model organism for toxicity testing. Larvae are characteristically cream in colour if alive and turn black when they die (Fig. 4). Fig. 5 shows the percentage of *Galleria mellonella* that were alive following injection with 10 μL of either 0.5 mg mL^{-1} of ZnO@ZIF-8, 1 mg mL^{-1} of ZnO@ZIF-8, 2 mg mL^{-1} of ZnO@ZIF-8 or sterile distilled water. Zero *Galleria mellonella* injected with 0.5 mg mL^{-1} of ZnO@ZIF-8, 2 mg mL ZnO@ZIF-8 or sterile distilled water had died by 72 h, whilst survival dropped to 90% after 48 h for the *Galleria mellonella* injected with 1 mg mL^{-1} ZnO@ZIF-8. Survival had decreased across all conditions by 96 hours, to a minimum of 70% survival (2 mg mL^{-1} ZnO@ZIF-8). These decreases in survival were considered not significant (P=0.5456) when comparing the survival data using a log-rank (mantel-cox) test, and therefore suggesting the ZnO@ZIF-8 compound was no more toxic to the *Galleria mellonella* at any of the tested concentrations when compared to distilled water.
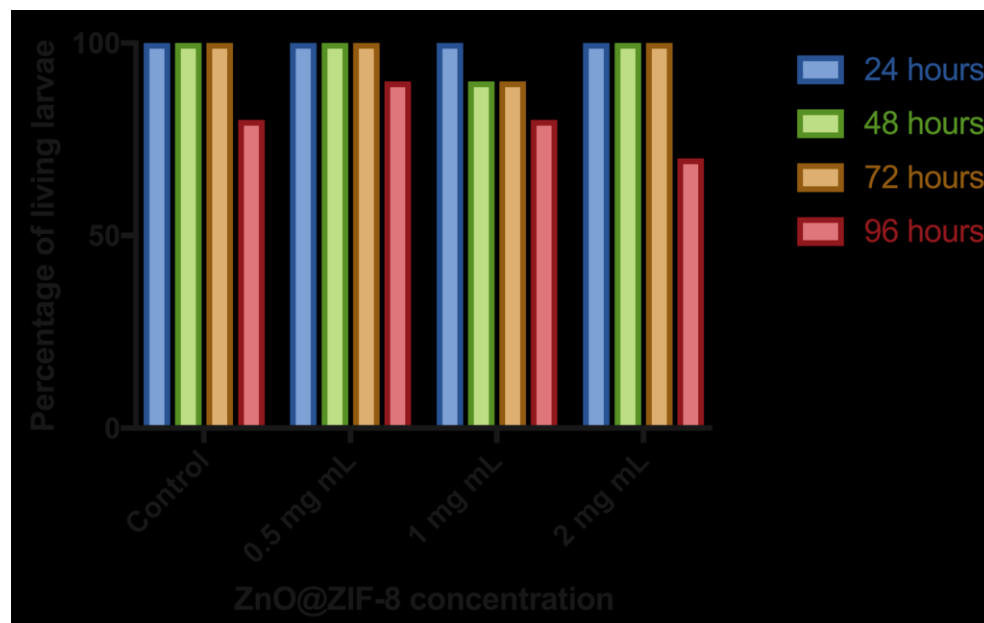
Figure 5. Survival of *Galleria mellonella* after injection with 10 µL of 2 mg mL^{-1}, 1 mg mL^{-1}, 0.5 mg mL^{-1} or 0.25 mg mL^{-1} of ZnO@ZIF-8 powder suspended in sterile distilled water. 10 µL of sterile distilled water was used as a control.

Efficacy of ZnO@ZIF-8 as an antibiofilm agent. ZnO@ZIF-8 reduced the number of viable cells in all bacterial biofilms to below the level of detection (BLD - a six to eight log decrease compared to exposure to control solution), over a 24-h period, at the highest tested concentration of 2 mg mL^{-1} (Fig. 6). Reduction to BLD was demonstrated at all three tested concentrations of ZnO@ZIF-8 after 3 h for *P. mirabilis* (six-log reduction) and *S. aureus* (seven-log reduction).
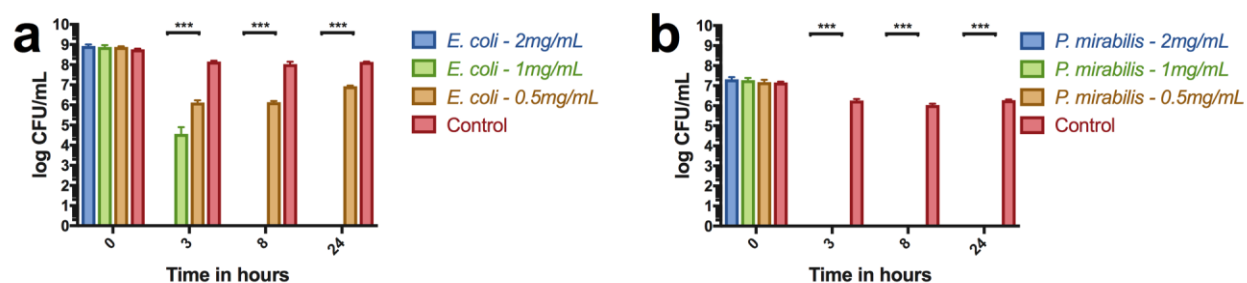
Figure 6. Number of colony forming units (living bacteria) recovered from each biofilm after treatment with ZnO@ZIF-8 powder suspended in sterile distilled water. Microorganisms tested were a) *E. coli*, b) *P. mirabilis*, c) *S. aureus* and d) *K. pneumoniae*.

For *E. coli*, the effect was concertation dependent, with 2 mg mL^{-1} ZnO@ZIF-8 reducing cell numbers BLD (eight-log drop) after three hours. 1 mg mL^{-1} ZnO@ZIF-8 reduced numbers by four-log within 3 h, and BLD by 8 h. 0.5 mg mL^{-1} was unable to reduce the biofilm below one-log within the 24 h test period. Whilst *K. pneumoniae* biofilms treated with 0.5 mg mL^{-1} and 1 mg mL^{-1} were not reduced BLD, they were able to provide a one and two-log decrease respectively. All colony forming unit counts were statistically significantly different ($p<0.001$ except 8 h - 1 mg mL^{-1} sample for *K. pneumoniae* which was significant to $p<0.05$) compared to the matched control biofilm, using a 2-way ANOVA statistical test.

The speed at which these biofilms and inocula on silicone are inactivated is of particular interest particularly when considering *P. mirabilis*. If left undisturbed in a catheter, this microorganism can produce urease, which increases the pH of the environment, leading to

crystalline deposits of calcium and magnesium phosphates, which can form encrustations and block the catheter. *P. mirabilis* has been shown to attach to catheter material within one hour, and produce diffuse crystalline deposits within four days.[46] If ZnO@ZIF-8 is able to stop or retard growth on silicone material, the effect on subsequent CAUTIs could be significant.

K. pneumoniae biofilms were the most resistant to ZnO@ZIF-8. Whilst these results are positive, they support the general observations that many *Klebsiella* species are known to produce a significant amount of biofilm matrix material, which enhances resistance to antimicrobial products and makes the removal of biofilm difficult. The strain of *K. pneumoniae* used in this study readily produces EPS, as can be seen in Fig. 7. Additionally, *K. pneumoniae* has been shown to produce more EPS when growing as a biofilm on silicone opposed to growing on other surfaces,[47] and thus further characterization of the antimicrobial effect of ZnO@ZIF-8 on such biofilms on catheter materials would be desirable.
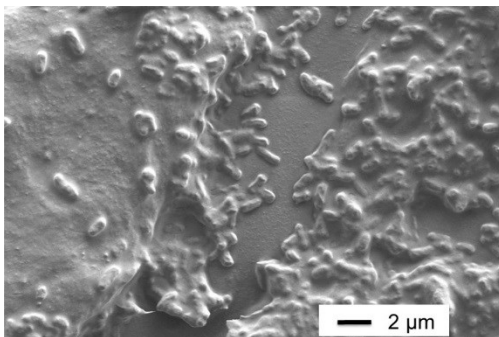

Figure 7. Scanning electron micrograph of *K. pneumoniae* in grown in biofilm on a silicone surface. Rod shaped cells are visible and embedded within the EPS produced by the cells.

3.3. Assessment of antimicrobial efficacy of ZnO@ZIF-8-containing silicone elastomers.
ZnO@ZIF-8 embedded in silicone demonstrated antimicrobial properties against all four test organisms. M511 maxillofacial SE embedded with 2 wt.% ZnO@ZIF-8 reduced *S. aureus* BLD

(five log decrease) within 3 h and reduced *E. coli* BLD by 8 h (five log decrease – silicone

figure). Both *P. mirabilis* and *K. pneumoniae* were reduced BLD within 24 h (six log decrease),

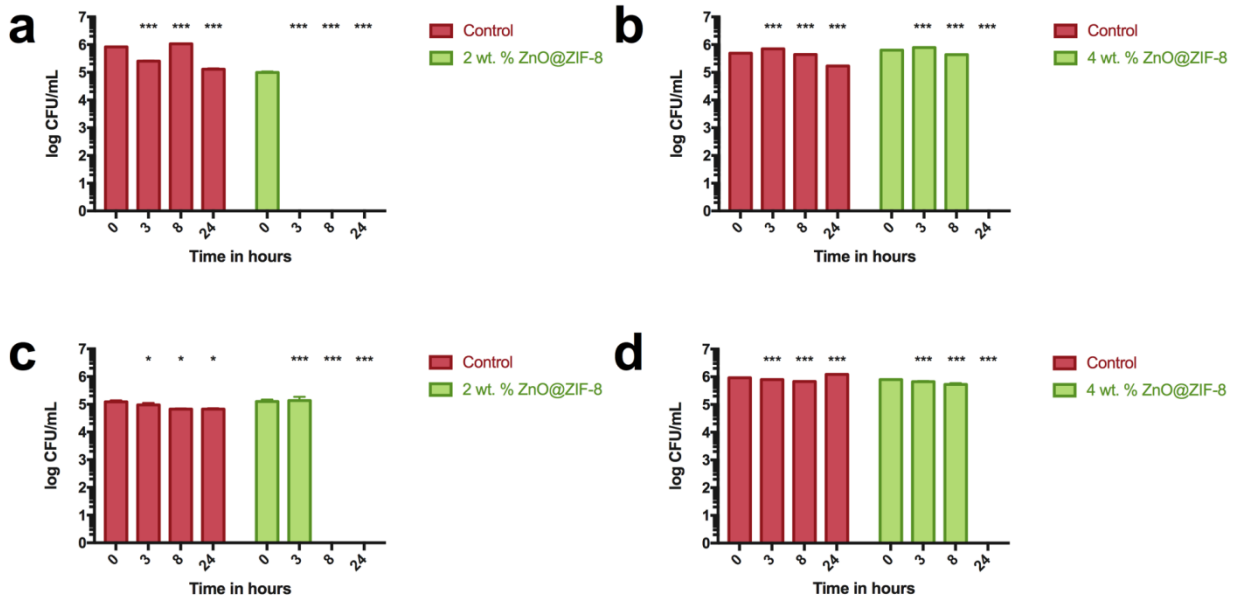when inoculated onto SE containing 4 wt.% (Fig. 8).

Figure 8. Number of colony forming units (living bacteria) recovered from silicone coupons

embedded with either 2 or 4 wt. % ZnO@ZIF-8 powder. Microorganisms tested were a) *E. coli*,

b) *P. mirabilis*, c) *S. aureus* and d) *K. pneumoniae*.

However, if cells are unable to survive on a catheter surface, then the likelihood of biofilm

formation is reduced. Although neither *K. pneumoniae* or *P. mirabilis* were eliminated from the

surface until 24 h, an effect was achieved. Both of these microorganisms were resistant overall to

the treatment of ZnO@ZIF-8 compared to *E. coli* and *S. aureus*, demonstrating variability of

susceptibility between microorganisms.

4. CONCLUSIONS

We have successfully optimized the synthesis procedure for the preparation of gram-scale phase pure ZnO@ZIF-8 composite. As a proof of concept, this study demonstrates the potential of ZnO@ZIF-8 composite as an antimicrobial additive to medical silicone devices such as catheters due to its ability to kill bacterial cells present on the surface of the silicone, as well as its promising anti-biofilm effect. This work also broadens the scope of MOF composite applications for widely applicable antimicrobial catheters. The results reported in this work, namely the ability of ZnO@ZIF-8 suspensions to reduce well-established microbial biofilms to beyond detection limit as well as the ability of ZnO@ZIF-8-embedded silicones to eliminate microorganisms from their surfaces, are significant for the quest to reduce catheter-associated urinary tract infections. Further work is in progress to investigate the ability of ZnO@ZIF-8-embedded silicones to inhibit biofilm growth as well as to establish the mechanism of antimicrobial action.

AUTHOR INFORMATION

Corresponding Author

*E-mail: l.tosheva@mmu.ac.uk (LT)

*E-mail: likhong.wee@kuleuven.be (LHW)

Author Contributions

The manuscript was written through contributions of all authors. All authors have given approval to the final version of the manuscript.

REFERENCES

(1) Magill, S. S.; Edwards, J. R.; Bamberg, W.; Beldavs, Z. G.; Dumyati, G.; Kainer, M. A.; Lynfield, R.; Maloney, M.; McAllister-Hollod, L.; Nadle, J.; Ray, S. M.; Thompson, D. L.; Wilson, L. E.; Fridkin, S. K. Multistate Point-Prevalence Survey of Health Care-Associated Infections. *New Engl. J. Med.* **2014**, *370*, 1198-1208.

(2) Saint, S.; Chenoweth C. E. Biofilms and Catheter-Associated Urinary Tract Infections. *Infect. Dis. Clin. North Am.* **2003**, *17*, 411-432.

(3) Lo, E.; Nicolle, L. E.; Coffin, S. E.; Gould, C.; Maragakis, L. L.; Meddings, J.; Pegues, D. A.; Pettis, A. M.; Saint S.; Yokoe, D. S. Strategies to Prevent Catheter-Associated Urinary Tract Infections in Acute Care Hospitals: 2014 Update. *Infect. Cont. Hosp. Ep.* **2014**, *35*, 464-479.

(4) Stickler, D. J. Bacterial Biofilms in Patients with Indwelling Urinary Catheters. *Nat. Clin. Pract. Urol.* **2008**, *5*, 598-608.

(5) *Global Priority List of Antibiotic-Resistant Bacteria to Guide Research, Discovery, and Development of New Antibiotics*. World Health Organization, 2017.

(6) Lawrence, E. L.; Turner, I. G. Materials for Urinary Catheters: A Review of Their History and Development in the UK. *Med. Eng. Phys.* **2005**, *27*, 443-453.

(7) Pickard, R.; Lam, T.; MacLennan, G.; Starr, K.; Kilonzo, M.; McPherson, G.; Gillies, K.; McDonald, A.; Walton, K.; Buckley, B.; Glazener, C.; Boachie, C.; Burr, J.; Norrie, J; Vale, L.; Grant, A.; N'Dow, J. Antimicrobial Catheters for Reduction of Symptomatic Urinary Tract Infection in Adults Requiring Short-Term Catheterisation in Hospital: A Multicentre Randomised Controlled Trial. *Lancet* **2012**, *380*, 1927-1935.

(8) Malic, S.; Jordan, R. P.; Waters, M. G.; Stickler, D. J.; Williams, D. W. Biocide Activity against Urinary Catheter Pathogens. *Antimicrob. Agents Ch.* **2014**, *58*, 1192-1194.

(9) Fisher, L. E.; Hook, A. L.; Ashraf, W.; Yousef, A.; Barrett, D. A.; Scurr, D. J.; Chen, X.; Smith, E. F.; Fay, M.; Parmenter, C. D.; Parkinson, R.; Bayston, R. Biomaterial Modification of Urinary Catheters with Antimicrobials to Give Long-Term Broadspectrum Antibiofilm Activity. *J. Control. Release* **2015**, *202*, 57-64.

(10) Ketchum, A. R.; Kappler, M. P.; Wu, J.; Chuanwu Xi, C.; Meyerhoff, M. E. The Preparation and Characterization of Nitric Oxide Releasing Silicone Rubber Materials Impregnated with S-Nitroso-Tert-Dodecyl Mercaptan. *J. Mater. Chem. B* **2016**, *4*, 422-430.

(11) Xu, L.-C.; Wo, Y.; Meyerhoff, M. E.; Siedlecki, C. A. Inhibition of Bacterial Adhesion and Biofilm Formation by Dual Functional Textured and Nitric Oxide Releasing Surfaces, *Acta Biomater.* **2017**, 51, 53-65.

(12) Goudie, M. J.; Jitendra Pant. J.; Handa, H. Liquid-Infused Nitric Oxide-Releasing (LINORel) Silicone for Decreased Fouling, Thrombosis, and Infection of Medical Devices, *Sci. Rep.* **2017**, *7*, 13623.

(13) Johnson, J. R.; Kuskowski, M. A.; Wilt, T. J. Systematic Review: Antimicrobial Urinary Catheters to Prevent Catheter-Associated Urinary Tract Infection in Hospitalized Patients. *Ann. Intern. Med.* **2006**, *144*, 116-126.

(14) Konstantelias, A. A.; Vardakas, K. Z.; Polyzos, K. A.; Tansarli, G. S.; Falagas, M. E. Antimicrobial-Impregnated and -Coated Shunt Catheters for Prevention of Infections in Patients with Hydrocephalus: A Systematic Review and Meta-Analysis. *J. Neurosurg.* **2015**, *122*, 1096-1112.

(15) Férey, G. Hybrid Porous Solids: Past, Present, Future. *Chem. Soc. Rev.* **2008**, *37*, 191-214.

(16) Farha, O. K.; Yazaydın, A. Ö.; Eryazici, I.; Malliakas, C. D.; Hauser, B. G.; Kanatzidis, M. G.; Nguyen, S. T.; Snurr, R. Q.; Hupp, J. T. De novo Synthesis of a Metal-Organic Framework Material Featuring Ultrahigh Surface Area and Gas Storage Capacities. *Nat. Chem.* **2010**, *2*, 944-948.

(17) He, Y.; Zhou, W.; Qian, G.; Chen, B. Methane Storage in Metal–Organic Frameworks. *Chem. Soc. Rev.* **2014**, *43*, 5657-5678.

(18) Li, J.-R.; Kuppler, R. J.; Zhou, H.-C. Selective gas adsorption and separation in metal–organic frameworks. *Chem. Soc. Rev.* **2009**, *38*, 1477-1504.

(19) Corma, A.; García, H.; Llabres i Xamena, F. X. Engineering Metal Organic Frameworks for Heterogeneous Catalysis. *Chem. Rev.* **2010**, *110*, 4606-4655.

(20) Kreno, L. E.; Leong, K.; Farha, O. K.; Allendorf, M.; Van Duyne, R. P.; Hupp, J. T. Metal–Organic Framework Materials as Chemical Sensors. *Chem. Rev.* **2012**, *112*, 1105-1125.

(21) Kohsari, I.; Shariatinia, Z.; Pourmortazavi, S. M. Antibacterial electrospun Chitosan-Polyethylene Oxide Nanocomposite Mats Containing ZIF-8 Nanoparticles. *Int. J. Biol. Macromol.* **2016**, *91*,778–788.

(22) Guo, Y-F.; Fang, W-J.; Fua, J.-R.; Wu, Y.; Zheng, J.; Gao, G-Q.; Chen, C.; Yan, R.-W.; Huang, S.-G.; Chun-Chang Wang. C. -C. Facile Synthesis of Ag@ZIF-8 Core-Shell Heterostructure Nanowires for Improved Antibacterial Activities. *Appl. Surf. Sci.* **2018**, *435*, 149–155.

(23) Horcajada, P.; Gref, R.; Tarek Baati, T.; Allan, P. K.; Maurin, G.; Couvreur, P.; Férey, G.; Morris, R. E.; Serre, C. Metal–Organic Frameworks in Biomedicine. *Chem. Rev.* **2012**, *112*, 1232–1268.

(24) Aguilera-Sigalat, J.; Bradshaw, D. Synthesis and Applications of Metal-Organic Framework-Quantum Dot (QD@MOF) Composites. *Coordin. Chem. Rev.* **2016**, 307, 267-291.

(25) Li, S.; Huo, F. Metal-Organic Framework Composites: From Fundamentals to Applications. *Nanoscale* **2015**, *7*, 7482-7501.

(26) Yang, Q.; Xu, Q.; Jiang, H.-L. Metal-Organic Frameworks Meet Metal Nanoparticles: Synergistic Effect for Enhanced Catalysis. *Chem. Soc. Rev.* **2017**, *46*, 4774-4808.

(27) Hosseinpour, S. A.; Karimipour, G.; Ghaedi, M.; Dashtian, K. Use of Metal Composite MOF-5-Ag$_2$O-NPs as an Adsorbent for the Removal of Auramine O Dye Under Ultrasound Energy Conditions. *Appl. Organomet. Chem.* **2018.** *32*, e4007.

(28) Liu, Y.; Li, S.; Zhang, X.; Liu, H.; Qiu, J.; Li, Y.; Yeung, K. L. New Membrane Architecture: ZnO@ZIF-8 Mixed Matrix Membrane Exhibiting Superb H$_2$ Permselectivity and Excellent Stability. *Inorg. Chem. Commun.* **2014**, *48*, 77-80.

(29) Vinogradov, A. V.; Zaake-Hertling, H.; Hey-Hawkins, E.; Agafonov, A. V.; Seisenbaeva, G. A.; Kessler, V. G.; Vinogradov, V. V. The First Depleted Heterojunction TiO$_2$–MOF-Based Solar Cell. *Chem. Commun.* **2014**, *50*, 10210-10213.

(30) Zhan, W.-W.; Kuang, Q.; Zhou, J.-Z.; Kong, X.-J.; Xie, Z.-X.; Zheng, L.-S. Semiconductor@Metal–Organic Framework Core–Shell Heterostructures: A Case of ZnO@ZIF-8 Nanorods with Selective Photoelectrochemical Response. *J. Am. Chem. Soc.* **2013**, *135*, 1926−1933.

(31) Wang, X.; Liu, J.; Leong, S.; Lin, X.; Wei, J.; Kong, B.; Xu, Y.; Low, Z.-X.; Yao, J.; Wang, H. Rapid Construction of ZnO@ZIF-8 Heterostructures with Size-Selective Photocatalysis Properties. *ACS Appl. Mater. Interfaces* **2016**, *8*, 9080–9087.

(32) Wee, L. H.; Janssens, N.; Sree, S. P.; Wiktor, C.; Gobechiya, E.; Fischer, R. A.; Kirschhock, C. E. A.; Martens, J. A. Local Transformation of ZIF-8 Powders and Coatings into ZnO Nanorods for Photocatalytic Application. *Nanoscale* **2014**, *6*, 2056-2060.

(33) Yi, G.-C.; Wang, C.; Park, W. I. ZnO Nanorods: Synthesis, Characterization and Applications. *Semicond. Sci. Tech.* **2005**, *20*, S22–S34.

(34) Jones, N.; Ray, B.; Ranjit, K. T.; Manna, A. C. Antibacterial Activity of ZnO Nanoparticle Suspensions on a Broad Spectrum of Microorganisms. *FEMS Microbiol. Lett.* **2008**, *279*, 71–76.

(35) Sirelkhatim, A.; Mahmud, S.; Seeni, A.; Kaus, N. H. M.; Ann, L. C.; Bakhori, S. K. M.; Hasan, H.; Mohamad, D. Review on Zinc Oxide Nanoparticles: Antibacterial Activity. and Toxicity Mechanism. *Nano-Micro Lett.* **2015**, *7*, 219–242.

(36) Seoane, B.; Coronas, J.; Gascon, I.; Benavides, M. E.; Karvan, O.; Caro, J.; Kapteijn, F.; Gascon, J. Metal–Organic Framework Based Mixed Matrix Membranes: A Solution for Highly Efficient CO_2 Capture? *Chem. Soc. Rev.* **2015**, *44*, 2421-2454.

(37) Kertik, A.; Wee, L. H.; Pfannmöller, M.; Bals, S.; Martens, J. A.; Vankelecom, I. F. J. Highly Selective Gas Separation Membrane Using In Situ Amorphised Metal–Organic Frameworks. *Energy Environ. Sci.* **2017**, *10*, 2342-2351.

(38) Tsai, C. J.-Y.; Loh, J. M. S.; Proft, T. Galleria Mellonella Infection Models for the Study of Bacterial Diseases and for Antimicrobial Drug Testing. *Virulence* **2016**, *7*, 214-229.

(39) Ceri, H.; Olson, M.; Morck, D.; Storey, D.; Read, R.; Buret, A.; Olson, B. The MBEC Assay System: Multiple Equivalent Biofilms for Antibiotic and Biocide Susceptibility Testing. *Methods Enzymol.* **2001**, *337*, 377-385.

(40) Fisher, L., Ostovapour, S.; Kelly, P.; Whitehead, K. A.; Cooke, K.; Storgårds, E.; Verran, J. Molybdenum Doped Titanium Dioxide Photocatalytic Coatings for use as Hygienic Surfaces: The Effect of Soiling on Antimicrobial Activity. *Biofouling* **2014**, *30*, 911-919.

(41) Park, K. S.; Ni, Z.; Côté, A. P.; Choi, J. Y.; Huang, R.; Uribe-Romo, F. J.; Chae, H. K.; O'Keeffe, M.; Yaghi, O. M. Exceptional Chemical and Thermal Stability of Zeolitic Imidazolate Frameworks. *PNAS* **2006**, *103*. 10186 –10191.

(42) Esken, D.; Noei, H.; Wang, Y.; Wiktor, W.; Turner, S.; Gustaaf Van Tendeloo, G.; Fischer. R. A. ZnO@ZIF-8: Stabilization of Quantum Confined ZnO Nanoparticles by a Zinc Methylimidazolate Framework and Their Surface Structural Characterization Probed by CO_2 Adsorption. *J. Mater. Chem.* **2011**, *21*, 5907-5915.

(43) Wiktor, C.; Meledina, M.; Turner, S.; Lebedev, O. I.; Fischer, R. A. Transmission Electron Microscopy on Metal–Organic Frameworks – A Review. *J. Mater. Chem. A* **2017**, *5*, 14969-14989.

(44) Ozkan, E.; Ozkan, F. T.; Allan, E.; Parkin. I. P. The use of zinc oxide nanoparticles to enhance the antibacterial properties of light-activated polydimethylsiloxane containing crystal violet. *RSC Adv*. **2015**, *5*, 8806-8813.

(45) L. Zhang, L.; Gowardman, J.; Rickard. C. M. Impact of microbial attachment on intravascular catheter-related infections. *Int. J. Antimicrob. Agents*, **2011**, *38*, 9-15.

(46) Wilks, S. A.; Fader M. J.; Keevil, C. W. Novel Insights into the Proteus mirabilis Crystalline Biofilm Using Real-Time Imaging. *PLoS One* **2015**, *10*, e0141711.

(47) Bandeira, M.; Borges, V.; Gomes, J. P.; Duarte, A.; Jordao L. Insights on Klebsiella pneumoniae Biofilms Assembled on Different Surfaces Using Phenotypic and Genotypic Approaches. *Microorganisms* **2017**, *5*, 16.

Table of contents

non-toxic

ZnO@ZIF-8

K. pneumoniae   S. aureus

E. coli   P. mirabilis

reduces established biofilm